

## APPLICATION OF COMPUTATIONAL FLUID DYNAMICS DIFFERENTIAL MODEL COUPLED WITH HUMAN THERMAL COMFORT INTEGRAL MODEL IN VENTILATED INDOOR SPACES

Eusébio Z. E. Conceição<sup>1</sup>, Daniel R. B. Geraldo<sup>1</sup> and M<sup>a</sup> Manuela J. R. Lúcio<sup>1</sup>  
<sup>1</sup>FCT-University of Algarve, Faro, Portugal

### ABSTRACT

In this study the coupling of computational fluid dynamics (CFD) differential and human thermal comfort (HTC) integral numerical models is developed and used. The HTC integral numerical model evaluates the thermal comfort in non-uniform environments, while the CFD differential numerical model evaluates the airflow inside the virtual chamber and around the manikins.

The numerical simulation, using upper crossed ventilation and made in winter conditions, is applied inside a virtual chamber equipped with two seated manikins, one desk and two seats. In this simulation the numerical airflow values, obtained with two different computational grid discretization with one and two manikins, are compared with experimental measurements.

### INTRODUCTION

In this work the evolution of thermal comfort level in an experimental and in a virtual chamber, equipped with crossed ventilation and occupied with one and two manikins is made. In this study two developed numerical models, based in coupling integral and differential numerical models are used.

In order to evaluate the thermal comfort level, the Predicted Mean Vote (PMV) and the Predicted Percentage of Dissatisfied people (PPD) indexes (based in the air temperature, air velocity, air relative humidity, Mean Radiant Temperature, clothing level and activity level) are used. These indexes were developed by Fanger (1970) and are presented in ISO 7730 (2005).

The PMV and PPD indexes developed previously for uniform environments, in this work are adapted and applied in non-uniform environments. This kind of methodology, also used by other authors as example in Miyanaga and Nakamo (1998), was developed, validated and applied in Conceição (1999), Conceição et al. (2006) and Conceição and Lúcio (2001). In the first and second ones were validated in uniform environments and in the third one was validated in non-uniform environments. In these last two works the human thermal comfort integral numerical model was used to evaluate the human thermal response when is subjected to a non-uniform forced airflow promoted by different local ventilators. In these works the air velocity and

temperature were obtained through experimental measurements.

Several authors applied the coupling of human thermal comfort integral numerical model and the computational fluid dynamics differential numerical model in some applications, as example Gau et al. (2006), Zhu et al. (2007) and Omni et al. (2007). The coupling of computational fluids dynamics and human body thermoregulation models for the assessment of personalized ventilation in the occupied space and in the breathing area were analysed in Gau et al. (2006). The coupling simulation method of convection, radiation, moisture transport and human thermal physiological model in the simulation of heat exchanges from a seated person, in an uniform environment, were analysed in Zhu et al. (2007). The coupling simulation of convection, radiation and thermoregulation for predicting human thermal sensation were analysed in Omni et al. (2007).

In the study presented in this work, the coupling of the human thermal comfort integral and of the computational fluid dynamics differential numerical models is used to evaluate the thermal comfort level, using the PMV and PPD indexes in non-uniform environment promoted by crossed ventilation with inlet and outlet located in adjacent walls.

### SIMULATION

#### **Numerical models**

In this work the human thermal comfort integral model and the computational fluid dynamics differential model is used in the evaluation of occupants' thermal comfort in non-uniform environments. The human thermal comfort integral numerical model, after the evaluation of the view factors between the human body sections and the surrounding surfaces, is used to evaluate the Mean Radiant Temperature, skin temperature, clothes temperature, transpired water and thermal comfort level (Predicted Mean Vote and Predicted Percentage of Dissatisfied people), in non-uniform environments. The computational fluid dynamics differential numerical model is used to evaluate the air velocity and air temperature field, around the manikin and inside the virtual chamber.

The non-uniform environment conditions are associated to the non-uniform airflow (air temperature and velocity) around the manikins and

associated to the non-uniform heat exchanges by radiation (surrounding surface temperatures). The computational fluid dynamics differential numerical model evaluates the first one, while the human thermal comfort integral numerical model evaluates the second one.

In order to evaluate the thermal comfort level, in the present methodology the airflow input used by the human thermal comfort integral numerical model is obtained by the computational fluid dynamics differential numerical model, while the surrounding conditions input used by the computational fluid dynamics differential numerical model to evaluate the airflow is obtained by the human thermal comfort integral numerical model. The computational fluid dynamics differential numerical model considers three boundary conditions: inlet airflow conditions (air velocity, air temperature and air turbulence intensity), surrounding room temperatures (wall, ceiling, floor and desk surfaces) and surrounding human body temperatures (skin and clothing surfaces). The human thermal comfort integral numerical model considers environmental variables around the occupant (air temperature and velocity) and the personal variables (clothing and activity levels).

In this work the coupling of the two numerical models is applied and in the numerical philosophy two steps and an iterative methodology is considered:

- In the first step, the computational fluid dynamics differential numerical model, using the body and clothing temperatures as boundary conditions around the manikin, is used to evaluate the environmental variables around the manikins.
- in the second step, the previous values are used as input data in the human thermal comfort integral numerical model, that calculates the body temperature and clothing temperature.
- In the numerical methodology, applying an iterative method and using sequentially the computational fluid dynamics differential numerical model in the first step and the human thermal comfort integral numerical model in the second step, the numerical methods stop when the convergence is guaranteed.

#### Human thermal comfort (HTC)

In the human thermal comfort integral numerical model, the human body and the clothing thermal response are based on energy balance integral equations and mass balance integral equations. In the resolution of these equations systems, the Runge-Kutta-Fehlberg method with error control is used.

In the human thermal comfort integral numerical model, the three-dimensional body is divided in 25 elements, each one is divided in 12 layers and each

one could be still protected from the external environment through some clothing layers. The developed composition of elements and layers (see Conceição et al. 2006), after other combinations being analysed, in accord to the validations tests and the time calculation, showed good results. This numerical model works in transient conditions and simultaneously simulates a group of persons in non-uniform conditions.

The human thermal comfort integral numerical model evaluates the:

- temperature of the body tissue, body skin and clothing;
- water vapour in the skin and in the clothing;
- Mean Radiant Temperature, that each body element is subjected;
- thermal comfort level, that each occupants is subjected.

The Mean Radiant Temperature is calculated based in the view factors, previously evaluated, calculated between the human body sections and the other human body sections and between the human body sections and the surrounding surfaces (internal desk, walls, door, ceiling and floor).

The human thermal comfort integral numerical model, before being used, was subjected to validation tests. In these validation tests experimental measurements and numerical results were compared. More details about these validation results can be seen, as example, in Conceição et al. (2006). Other application examples about this numerical model can be seen, as example, in Conceição et al. (2006), Conceição et al. (2010a) and Conceição et al. (2010b). In the last two works the thermal comfort level was evaluated in personalized ventilation equipped with an air terminal device localised above the writing desk and another air terminal device localised below the writing desk. In Conceição et al. (2010a) only the airflow around the occupants was analysed, while in Conceição et al. (2010b) also the airflow inside the chamber was analysed.

The thermal comfort, that is associated to all the body, in this model considers the heat exchange contribution between all human body sections and the environment and the internal heat generation gain. In the previous studies, made by the same authors, the information obtained by the computational fluid dynamics differential numerical model around the occupants was not considered, while in this work this information is considered.

#### Computational fluid dynamics (CFD)

The computational fluid dynamics differential numerical model simulates the three-dimensional turbulent airflow, in steady-state regimen and in non-isothermal conditions, inside an occupied space.

The numerical model, in Cartesian coordinates domain, is based in partial differential equations. In these partial differential equations discretization the

finite volume method is used, in the equations system resolution an iterative TDMA method is considered, in the convective and diffusive fluxes the hybrid scheme is applied, in the velocity and pressure equations the SIMPLE algorithm is used, in the surfaces proximity the wall boundary is considered, in the vertical air velocity equation the impulsion term is applied, in the computational grid discretization an uniform methodology is considered and in the turbulence simulation the RNG turbulence model is used. See more details in Patankar (1980).

The computational fluid dynamics numerical model evaluates the:

- air velocity;
- air temperature;
- air pressure;
- turbulent kinetic energy;
- turbulent energy dissipation rate;
- carbon dioxide concentration.

In this study a correction presented in Popiolek and Melikov (2004) is used in the air velocity numerical values.

Some computational fluid dynamics numerical model validation tests were made, in steady-state regimen in isothermal conditions (see Conceição et al., 2008) and in non-isothermal conditions, (see Conceição et al., 2010b). In Conceição et al. (2008) the airflow inside the experimental chamber without occupation was considered, while in Conceição et al. (2010b) the airflow inside the experimental chamber with occupation of a higo-thermal manikin was analysed.

### Numerical methodology

The human thermal comfort integral numerical model considers the human body divided in cylinders and sphere (see figure 1a). In the surrounding surfaces, in each cylinder and sphere a numerical computational grid discretization of  $8 \times 8$  is considered, while in each surrounding building surfaces a numerical computational grid discretization of  $10 \times 10$  is considered. This numerical computational grid discretization is used in the view factors determination, namely, in the view factors between:

- the human body sections and the other human body sections (not only for the other human bodies but also for the own body);
- the human body sections and the surrounding buildings surfaces.

The computational fluid dynamics numerical model considers two computational grid discretization:

- a  $48 \times 56 \times 48$  computational grid discretization: 5.45 cm spaced in X direction, 5.2 cm spaced in Y direction and 5.45 cm spaced in Z direction;
- a  $96 \times 112 \times 96$  computational grid discretization: 2.725 cm spaced in X

direction, 2.6 cm spaced in Y direction and 2.725 cm spaced in Z direction.

The manikins and the interior bodies (desk and seats) are developed using boxes with similar numerical computational grid discretization (see figure 1b).

The virtual manikins considered in the numerical simulation, had 1.70 m of height, 70 Kg of weight, 1.2 Met. of activity level and 1 Clo. of clothing level (equal to the higo-thermal manikin).

The air temperature, the air velocity and the Mean Radiant Temperature around the manikins are numerically calculated. The first and second ones are calculated through the computational fluid dynamics differential numerical model, while the third one is calculated through the human thermal comfort integral numerical model.

The mean air relative humidity, used in this numerical simulation, is experimentally measured.

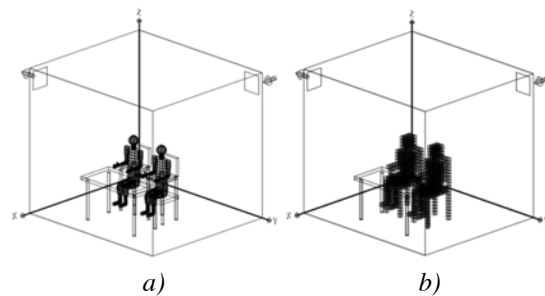


Figure 1 Virtual numerical human bodies considered in the human thermal comfort integral numerical model a) and in the computational fluid dynamics differential numerical model b).

In figure 2 the vertical and horizontal plans located at  $X=130$  cm,  $Y=110$  cm,  $Y=170$  cm and  $Z=120$  cm, when the  $48 \times 56 \times 48$  computational grids are used are presented. The figure a) considers one manikin, while the figure b) considers two manikins.

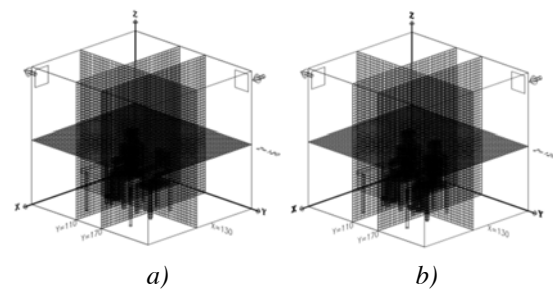


Figure 2 Representation of the plans located at  $X=130$  cm,  $Y=110$  cm,  $Y=170$  cm and  $Z=120$  cm, when one a) and two b) manikins are used.

### EXPERIMENTAL SETUP

In this work one wooden experimental chamber with  $2.7 \times 2.4 \times 2.4$  m<sup>3</sup>, equipped with one desk, one seat and one seated higo-thermal manikin are used. The airflow simulated in this work, in the experimental chamber, is promoted by a crossed ventilation

philosophy, with the inlet and the outlet located above the head level. The inlet is localized in the back wall, on the left side of the seated higo-thermal manikin, while the outlet is localized in the right wall, on the right side of the seated higo-thermal manikin. The higo-thermal manikin used to simulate the occupant's posture in the experimental chamber, is able to simulate the occupant's body posture and the latent and sensible heat exchanges. In Conceição et al. (2010a) and Conceição et al. (2010b) are presented more details about this manikin. In Conceição et al. (2010a) and Conceição et al. (2010b) a combination of experimental measurements and numerical results were applied, when a personalised ventilation system is used.

In this work the experimental tests are made in steady state regimen, with non-isothermal conditions. Before obtaining the steady state regimen, the crossed ventilation and the sweating higo-thermal manikin works during several hours. When the steady state conditions are obtained, namely the thermal equilibrium between the higo-thermal manikin and the environment, the environmental variables are measured.

The indoor climate analyser BABUC-A (using sensors from LSI), multi-data logger with 11 inputs, is used to measure the mean environmental variables inside the experimental chamber, namely the air relative humidity, temperature, turbulence intensity and velocity and the surrounding surfaces temperatures.

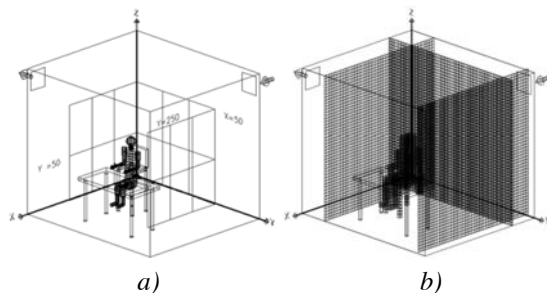


Figure 3 Representation of vertical plans located at  $X=50$  cm,  $Y=50$  cm and  $Y=250$  cm, for one manikin. Experimental a) and numerical b) vertical plans.

Table 1

Inlet and surrounding conditions obtained in the experimental tests and used in the numerical simulations.

Inlet conditions	Measured values
Inlet air velocity	2.5 m/s
Inlet air temperature	15 °C
Inlet air turbulence	10 %

Surrounding conditions	Measured values
Floor surface temperature	18.0 °C
Ceiling surface temperature	18.0 °C
Wall surface temperature	18.0 °C
Interior bodies temperature	18.0 °C

In table 1 the inlet and surrounding conditions obtained in the experimental tests, and used in the numerical tests, are presented.

In the numerical model validation tests the air velocity field measured and calculated in three vertical plans, located around the higo-thermal manikin, are compared (see figure 3). In the figure 3a the vertical plans show the locations where the experimental measurements are made, where in figure 3b the vertical plans show the locations where the numerical calculation are made.

## DISCUSSION AND RESULT ANALYSIS

In this section the numerical model validation, the airflow around the manikins and the thermal comfort level evaluations are made.

In the experimental tests one occupant (one higo-thermal manikin) is considered, while in the numerical tests one and two occupants (virtual manikins) are considered. In the validation the air velocity numerical results and experimental measurements are compared, when only one manikin is considered.

In the computational fluid dynamics numerical simulation the results of two computational grid discretization are compared.

### Numerical model validation

In figure 4 the air velocity field, in the vertical plan  $Y=250$  cm, obtained experimentally and numerically are presented and compared. In the figure a) the experimental measurements are presented, while in figures b) and c) the numerical results are showed: in the figures b) the  $48 \times 56 \times 48$  computational grid discretization are used, while in the figures c) the  $96 \times 112 \times 96$  computational grid discretization are used.

In accordance with the obtained results is verified that, in the experimental measurements and in the numerical results, the air velocity in the plan  $X=50$  cm and in the plan  $Y=50$  cm, in general, is around 0.4 m/s. In the plan  $Y=250$  cm the air velocity in the occupied area is, in general, around 0.4 m/s and in the upper area the air velocity increases.

It is verified that the numerical results are in accordance with the experimental measurements and the numerical results obtained in the  $48 \times 56 \times 48$  computational grids discretization and in the  $96 \times 112 \times 96$  computational grid discretization are similar. Thus, as the simulations with  $96 \times 112 \times 96$  computational grid discretization needs more time calculation, in this work the  $48 \times 56 \times 48$  computational grid discretization is used. Around the manikins, in the occupied space, the measured data and the calculated values are in accordance. However, in the upper inlet jet central area the measured results are slightly higher than the calculated values.

Some verified discrepancies, between the numerical results and the experimental measurements, are

associated to the grid discretization used in the virtual manikin, seat and desk and with the not consideration in the numerical model of the traversing system and measuring equipment used in the experimental tests. In the computational fluid dynamics differential model boxes are considered and in the human thermal comfort integral numerical model cylinders and sphere are considered.

**Airflow inside the virtual chamber**

In this section the airflow inside the virtual chamber and around the manikins, namely the air velocity (figure a) and air temperature (figure b), are presented in figure 5 (when one manikin is used) and in figure 6 (when two manikins are used). The vertical plans located at X=130 cm (with the sub index 1), Y=110 cm (with the sub index 2), Y=170 cm (with the sub index 3) and Z=130 cm (with the sub index 4) are presented.

In the airflow inside the experimental chamber and around the manikin two main areas are identified: an inlet jet area and a recirculation area. The inlet jet area is located above the occupants head level in the left side and in the front area, while the recirculation influenced area is located behind the occupants area.

In accordance with the obtained results, no significant air velocity field difference is verified when one or two manikins are used. In general, the air velocity is lower around the manikins than far from the manikins. Highest air velocity values are verified in the inlet jet area.

The air temperature is higher when two manikins are used than when only one manikin is used. In general, the air temperature is highest around the manikins and is lowest mainly in the inlet and in the recirculation area. The pictures also show the convection airflow promoted by the lower limbs.

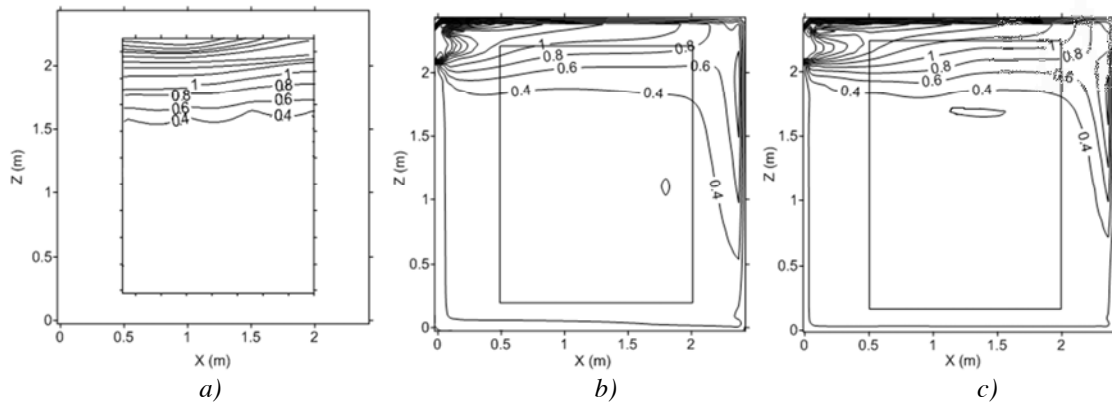


Figure 4 Comparison between numerical and experimental results of the vertical plan Y=250 cm is presented. In figure a) the experimental results are presented, in figure b) the numerical values in the 48x56x48 computational grid discretization are showed and in figure c) the numerical values in the 96x112x96 computational grid discretization are presented.

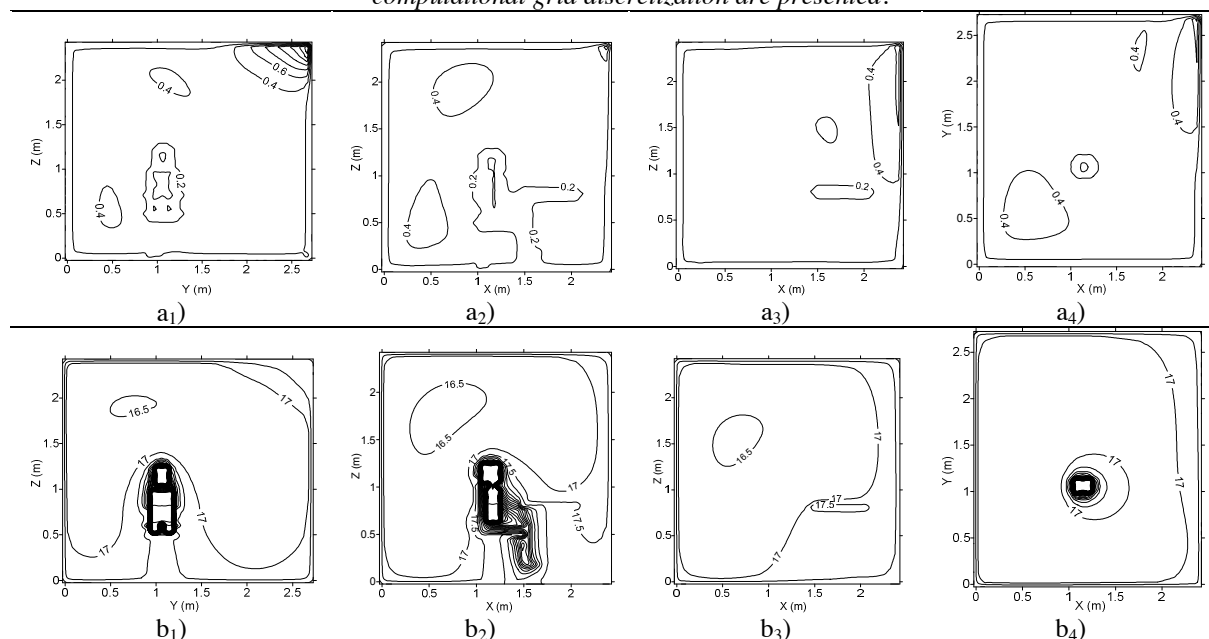


Figure 5 Numerical results of air velocity a) and air temperature b) fields in vertical plans located at X=130 cm (with the sub index 1), Y=110 cm (with the sub index 2), Y=170 cm (with the sub index 3) and Z=130 cm (with the sub index 4), for one manikin.

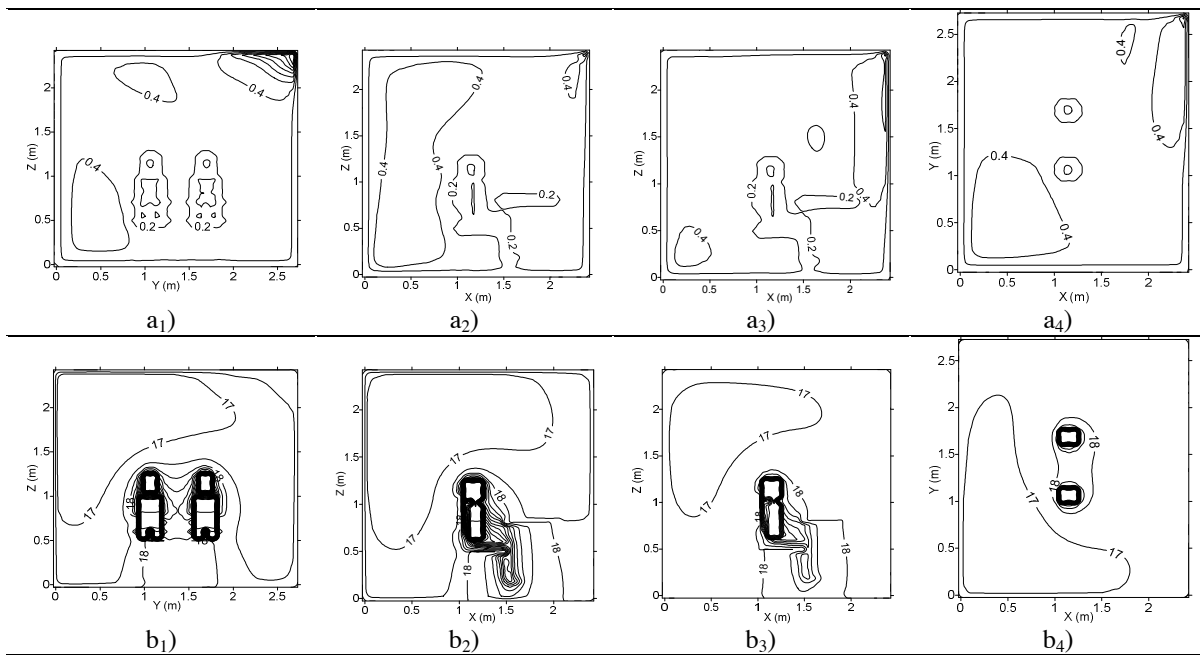


Figure 6 Numerical results of air velocity a) and air temperature b) fields in vertical plans located at  $X=130$  cm (with the sub index 1),  $Y=110$  cm (with the sub index 2),  $Y=170$  cm (with the sub index 3) and  $Z=130$  cm (with the sub index 4), for two manikins.

**Thermal comfort level**

In this section the thermal comfort level, when one and two manikins are used is evaluated. The air velocity, air temperature, Mean Radiant Temperature and the human body skin temperature are previously evaluated.

In figure 7 and 8 the calculated air velocity around the different body sections are presented, respectively, when one and two manikins are used. The calculated air temperature around the different sections are presented when one and two manikins are used, respectively, in figures 9 and 10.

In figure 11 and 12 the calculated Mean Radiant Temperature, that each body sections is subjected, are presented, respectively, when one and two manikins are used. The calculated skin temperature in the different human body sections is presented when one and two manikins are used, respectively, in figures 13 and 14.

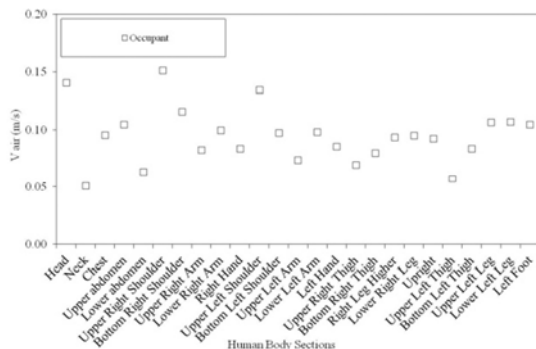


Figure 7 Numerical air velocity around one manikin seated in the right side.

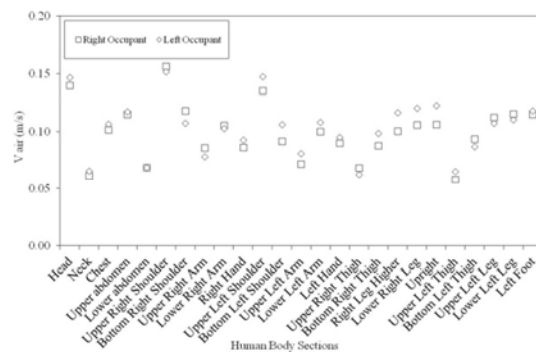


Figure 8 Numerical air velocity around two manikins seated in the right and left side.

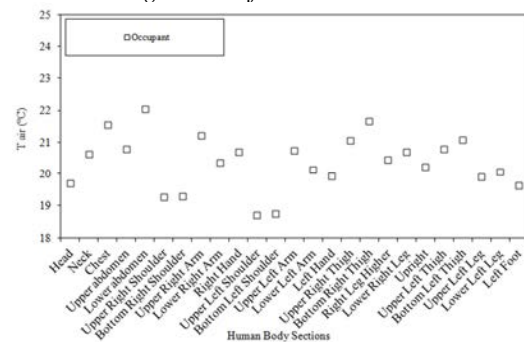


Figure 9 Numerical air temperature around one manikin seated in the right side.

Finally, the thermal comfort level, that the manikins are subjected, is presented in table 2 and 3, respectively, when one and two manikins are used. In these tables, the PMV and the PPD values are presented.



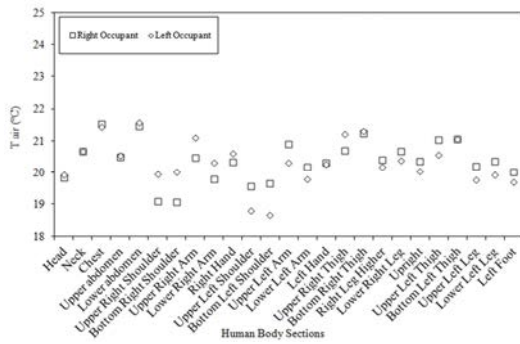


Figure 10 Numerical air temperature around two manikins seated in the right and left side.

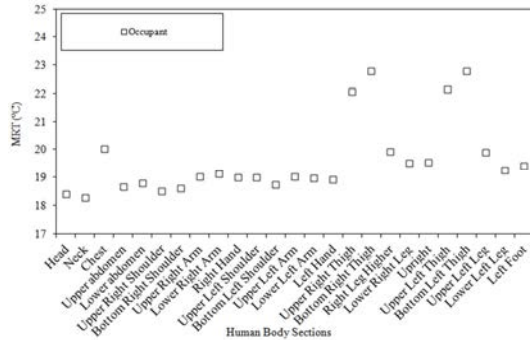


Figure 11 Numerical Mean Radiant Temperature, that each body sections is subjected, in one manikin seated in the right side.

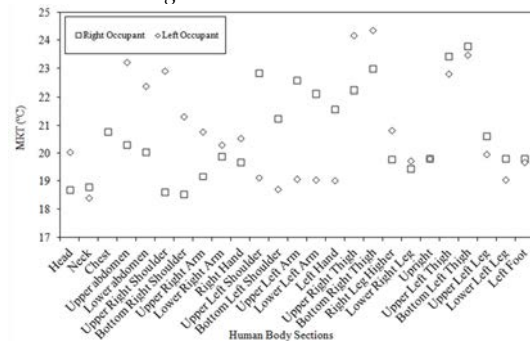


Figure 12 Numerical Mean Radiant Temperature, that each body sections is subjected, in two manikins seated in the right and left side.

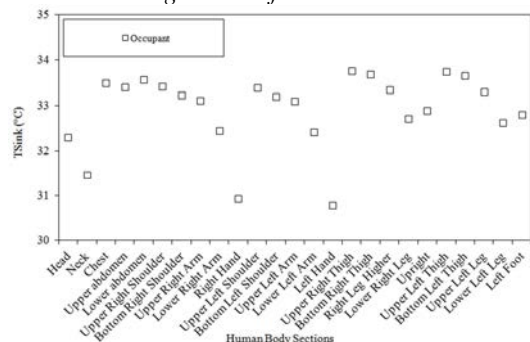


Figure 13 Numerical skin temperature in one manikin seated in the right side.

In general the air velocity field around the manikins is relatively uniform. However, when two manikins are used the air velocity around the left side seat manikin is slightly higher than the air velocity around the right side seat manikin.

The air temperature around the manikins is quite uniform. When two manikins are used the air temperature around the manikins is lightly higher than when only one manikin is used.

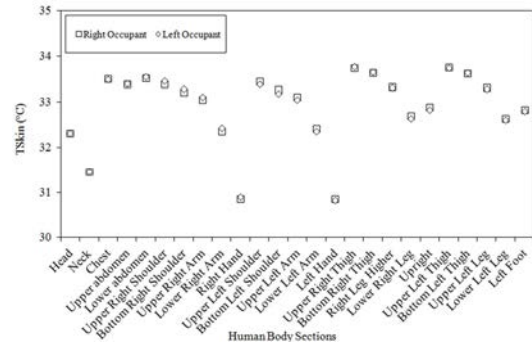


Figure 14 Numerical skin temperature in two manikins seated in the right and left side.

The Mean Radiant Temperature values are higher when two manikins are used than when only one manikin is used. When two manikins are used, in the left side seat manikin, the right limbs Mean Radiant Temperature is higher than the left limbs Mean Radiant Temperature, due to the heat exchange by radiation between manikin's body sections. In the right side seat manikin the opposite is verified.

The skin temperature is highest in the trunk area and decreasing along the upper and lower limbs (clothed area). The hands (non-clothed area) present the lowest skin temperature values.

Table 2

Thermal comfort level, when one manikin is used.

Manikin	PMV	PPD
Right	-0.30921	6.987216

Table 3

Thermal comfort level, when two manikins are used.

Manikin	PMV	PPD
Left	-0.23607	6.156411
Right	-0.08315	5.143173

Finally, the thermal comfort level in both situations is acceptable, by negative PMV values, in accordance with the ISO 7730 (2005). However, when two manikins are used, due to the increase of the internal air temperature, the thermal comfort levels slightly increase.

## CONCLUSIONS

The thermal comfort level, that one and two seated occupants are subjected in spaces equipped with crossed ventilation in winter environments, is evaluated in this work. A combination of experimental tests and numerical simulations and coupling integral and differential numerical models are used.

The crossed ventilation is guaranteed with inlet and the outlet placed above the head level in adjacent walls. This airflow topology promotes two areas: the non-occupied upper area (which contains the airflow inlet and outlet) with high air velocity levels and the occupied lower area with low air velocity levels.

In accordance with the obtained results is verified that the numerical values are in accordance with the experimental measurements. Some verified discrepancies are associated to the grid discretization applied in the virtual manikins, seat and desk (boxes used in the computational fluid dynamics differential numerical model and cylinders and sphere used in the human thermal comfort integral numerical model) and with the not consideration in the numerical simulation of the traversing system and experimental equipment.

In the airflow inside the experimental chamber and around the manikin an area influenced by the inlet jet (located above the occupants head level in the left and in front side) and a recirculation area (located behind the occupants) are identified. In general, the air velocity is lowest around the manikins and highest in the inlet area. In general, the air temperature is highest around the manikins (due the convection airflow) and is lowest mainly in the inlet and in the recirculation area.

The air velocity and temperature field around the manikins are relatively uniform. When two manikins are used the air velocity and the air temperature around the manikins, in general, slightly increase.

The Mean Radiant Temperature values are higher when two manikins are used than when only one manikin is used. The skin temperature is highest in the trunk area, decreasing along the upper and lower limbs (clothed area) and is lowest in the hands area (non-clothed area).

When only one manikin is used, the thermal comfort level is acceptable by negative PMV values. However, when two manikins are used the thermal comfort level is acceptable, also by negative PMV values, but with best thermal comfort levels.

## REFERENCES

Bulinska, A. 2007. Determination of Airflow Pattern in a Residential Building Using Metabolic Carbon Dioxide Concentration Measurements. RoomVent'2007, Helsinki, Finland, 13-15 June 2007.

Conceição E. Z. E. and Lúcio M<sup>a</sup> M. J. R. 2001. Numerical and subjective responses of human thermal sensation. Proceedings of the BioEng 2001 - Sixth Portuguese Conference on Biomedical Engineering, Faro, Portugal.

Conceição E. Z. E., Lúcio M<sup>a</sup> M. J. R., Capela T. L. and Brito A. I. P. V. 2006. Evaluation of thermal comfort in slightly warm ventilated spaces in non-uniform environments. Int. Journal of Heating, Ventilating, Air-Conditioning and Refrigerating Research, ASHRAE, Vol. 12, N. 3, pp. 451-458.

Conceição E. Z. E., Lúcio M<sup>a</sup> M. J. R., Rosa S. P., Custódio A. L. V., Andrade R. L. and Meira M<sup>a</sup> J. P. A. 2010b. Evaluation of comfort level in desks equipped with two personalized ventilation systems in slightly warm environments. Building and

Environment, Volume 45, Issue 3, March 2010, pp. 601-609.

Conceição E. Z. E., Rosa S. P., Custódio A. L. V., Andrade R. L., Meira M<sup>a</sup> J. P. A. and Lúcio M<sup>a</sup> M. J. R. 2010a. Study of Airflow Around Occupants Seated in Desks Equipped With Upper and Lower Air Terminal Devices for Slightly Warm Environments, Int. Journal on Heating Air Conditioning and Refrigerating Research, ASHRAE, Vol. 16, N. 4, July 2010, pp. 401-412.

Conceição, E. Z. E. 1999. Avaliação de condições de conforto térmico: simulação numérica do sistema térmico do corpo humano e do vestuário. In: Proceedings of the CIAR'99 - V Ibero and Inter-American Air Conditioning and Refrigeration Congress, Lisbon, Portugal.

Conceição, E. Z. E., Vicente, V. D. S. R. and Lúcio. M<sup>a</sup> M. J. R. 2008. Airflow inside school buildings office compartments with moderate environment. Int. Journal on Heating Air Conditioning and Refrigerating Research, ASHRAE, Vol. 14, N. 2, March 2008, pp. 195-207.

Fanger P.O. 1970. Thermal comfort. Copenhagen: Danish Technical Press.

Fanger, P. O. and Christensen, N. K. 1986. Prediction of Draught in Ventilated Spaces, Ergonomics, V. 29, pp. 215-235.

Gau, N., Niu J. and Zang, H. 2006. Coupling CFD and Human Body Thermoregulation Model for the Assessment of Personalized Ventilation. International Journal of Heating, Ventilating, Air-Conditioning and Refrigerating Research, ASHRAE, Vol. 12, N. 3, pp. 497-518.

ISO 7730, 2005. Ergonomics of the thermal environments – analytical determination and interpretation of thermal comfort using calculation of the PMV and PPD indices and local thermal comfort criteria. International Standard. Switzerland.

Miyanaga, T. and Nakamo Y. 1998. Analysis of thermal sensation in a radiant cooled room by modified PMV. RoomVent 1998, KTH, Stockholm, Sweden.

Omni, O and Tenabe, S. 2007. Coupled Simulation of Convection-Radiation-Thermoregulation for Predicting Human Thermal Sensation. RoomVent'2007, Helsinki, Finland, 13-15 June 2007.

Patankar, S.V. 1980. Numerical heat transfer and fluid flow. Hemisphere publishing corporation.

Popiolek, Z. and Melikov, A. 2004. Improved interpretation and validation of CFD predictions, RoomVent 2004, Coimbra, Portugal.

Zhu, S., Kato, S., Ooka, R., Sakoi, T. and Tsuzuki, K. 2007. Coupled Simulation Method of Convection, Radiation, Moisture Transport and Sakoi Human Thermal Physiological Model to Simulate Heat Exchange from a Person Seated in a uniform environment. RoomVent'2007, Helsinki, Finland, 13-15 June 2007.